

## Article

# Hydraulic Jump Behavior during Filling Process of Cast Start I

Jin Chen \*, Lei Zhang, Jiageng Zhang, Pan Cui, Guowei Luan and Fei Wang

Key Laboratory of Electromagnetic Processing of Materials (Ministry of Education), Northeastern University, Shenyang 110004, China

\* Correspondence: chenjin@epm.neu.edu.cn; Tel.: +86-24-83681733

**Abstract:** This paper presents a 0.25 scale quasi-three-dimensional hydraulic model experiment of transient fluid flow phenomena during continuous casting of steel. The relationship between the continuous casting process and the hydraulic jump phenomenon is established. The casting process in the mold is divided into four stages (I–IV) from the beginning to the end of continuous casting. The filling process involves stages I–II and is investigated by high-speed camera. The filling process is part of the cast start. In this paper, the hydraulic jump behavior varies and is controlled by different spring and iron chips arrangement on the dummy bar during the filling process. A filling coefficient is proposed to judge the best filling conditions and apply them to the whole filling process. There is an optimal spring and iron chip arrangement, which can adjust the hydraulic jump to optimize the initial flow field during the filling process, even the whole continuous casting process.

**Keywords:** hydraulic jump; cast start; spring and iron chip arrangement; dummy bar



**Citation:** Chen, J.; Zhang, L.; Zhang, J.; Cui, P.; Luan, G.; Wang, F. Hydraulic Jump Behavior during Filling Process of Cast Start I. *Metals* **2022**, *12*, 1489. <https://doi.org/10.3390/met12091489>

Academic Editor: Noé Cheung

Received: 2 August 2022

Accepted: 7 September 2022

Published: 8 September 2022

**Publisher's Note:** MDPI stays neutral with regard to jurisdictional claims in published maps and institutional affiliations.



**Copyright:** © 2022 by the authors. Licensee MDPI, Basel, Switzerland. This article is an open access article distributed under the terms and conditions of the Creative Commons Attribution (CC BY) license (<https://creativecommons.org/licenses/by/4.0/>).

## 1. Introduction

In the continuous casting process, the flow field in the mold influences the quality of the final product by affecting the solidification of molten steel, temperature distribution, inclusions, and solution distribution in the mold. If the flow field fluctuates too much, it will cause quality defects of the billet [1–3]. Therefore, obtaining the law of the flow field in the mold and designing appropriate control parameters is the key to improving the quality of the billet. Some scholars believe that the physical properties of water are different from those of liquid metals, which cannot fully simulate the actual production conditions, such as the electromagnetic field [4,5]. However, due to the convenience and cost-effectiveness of water, the visual water model experiment is an important method to study the flow field in a metallurgical process [6–12], and its results can effectively guide the actual production after long-term verification in the metallurgical industry. The qualitative observation of tracers is the most common in water model experiments [6–8], and the results of PIV [10,11] and UDV [6] are both good in quantitative observation methods. UDV can also be used for the measurement of the opaque fluid flow field [4,5]. Some of these studies have observed the full-field velocity of the mold, and others mainly focused on the fluctuation of the liquid level or velocity changes in a specific area. They all concluded that the large fluctuation of the flow field in the mold would cause problems, such as slag entrainment, leading to the defects of billets. Additionally, the amount of inclusions is much larger during casting variation than during steady casting [13–15]. Casting variation states during continuous casting of steel include cast start, cast end, steel grade change, regular casting speed change, and cast fluctuations induced by certain reasons, such as nozzle clogging, which can result in defects, poor quality, and even breakout, involving ladle, tundish, mold, and other equipment [13–17]. The head billets, even the first three billets in some cases, often fail to meet the requirements. Further, 80% of surface defects in continuous casting billets originate from the mold [3], in which most inclusions and bubbles are generated and difficult to remove during casting variation states. Therefore, it is necessary to remove the bubbles and inclusions during casting variation states, especially

the cast start. However, the cast variation states, especially the cast start, have received relatively little attention [13–15].

In order to better analyze the flow field in the mold during the cast start, the process of cast start is described here. It includes the filling process and the dragging of a dummy bar. The dummy bar is inserted into the mold before casting to prevent the molten steel from moving out directly. Spring and iron chips are usually laid on the dummy bar to avoid the direct contact of molten steel and promote the molten steel to form a shell during the cast start. Meanwhile, the casting process in the mold is divided into four stages (I–IV) from the beginning to the end of continuous casting (shown in Figure 1): I—in the cast start process, after laying springs and iron chips on the dummy bar, the jet impinging on the spring and iron chip, the liquid level in the mold is extremely low, that is, the beginning of the filling process; II—the liquid level gradually rises until it reaches the immersion depth, the dummy bar is dragged during this process, that is, the filling process and the dragging of a dummy bar; III—the steady-state stage, the liquid surface is kept at the immersion depth and the continuous casting is carried out stably; IV—the end stage of continuous casting, the liquid level continues to drop until the cast end. During the whole continuous casting, the flow field in the mold is inseparable from the hydraulic jump phenomenon in fluid mechanics. The relationship between the hydraulic jump and continuous casting process is established. The details are as follows:

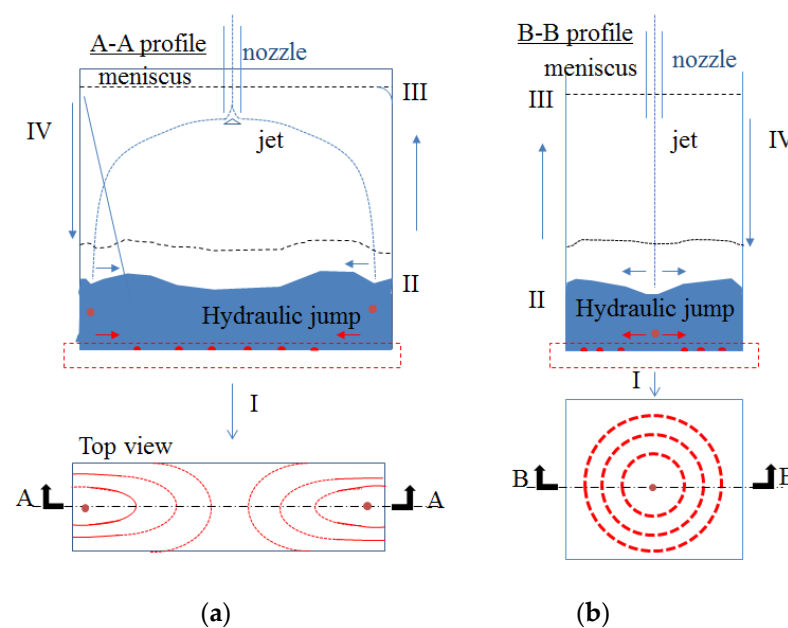


**Figure 1.** Hydraulic jump in the continuous process in the mold; (a) slab (b) bloom. (A-A profile is the profile at the centerline of the top view).

In stage I, a circular hydraulic jump (CHJ) occurs first (the red arc in the top view of Figure 1 is a schematic representation of the circular hydraulic jump; it is a shallow fluid hydraulic jump). If there is no boundary, the surface tension plays a leading role at this time, and the surface tension and viscous force are balanced with the momentum of the water film, although gravity does not play a significant role in it (the criterion formula for judgment is  $1/We + 1/Fr^2 = 1$ ,  $We$  is the Weber number, and  $Fr$  is Froude number) [18]; If there is a boundary, then the flow can quickly reach a steady state, and at this time, the formation of the hydraulic jump is dominated by gravity (common stationary hydraulic jump) [19,20]. Stages I and II are studied in this paper, three physical forms of hydraulic jump in and not in the mold is given: 1st forms—after the jet hits the bottom surface, the circular hydraulic jump starts, the center of the mold is a cavity and a very thin liquid film here, that is, the surface flow (seen in Figure 2; photos in Figures 6 and 8); that is, the initial

formation of a circular hydraulic jump, in which the flow downstream of the jump has not yet arrived at the outlet boundary (it is the mold wall if in the mold), is called a developing jump. Once the flow downstream of the jump arrives at the outlet boundary (not in the mold or low wall), the flow downstream of the jump falls uniformly down from the outlet boundary, and is called a developed jump, the steady-state CHJ, the whole process is a shallow fluid hydraulic jump [19]. In the filling process, there is a very high boundary (the wall of the mold), and the flow cannot get over it, that is, no downstream exists as the developed jump, no longer a shallow fluid hydraulic jump. After the flow arrives at the wall, then it is blocked and comes back to the center of the mold. The circular hydraulic jump begins to disappear at the moment, which is hereafter called CHJ. The 2nd form—the CHJ disappears and transforms to a common stationary hydraulic jump (hydraulic jump transition begins, it is gradually dominated by gravity), then flows back to the center and fills up the cavity formed by the hydraulic jump. At the moment in stage II, CHJ completely disappears, then a common stationary hydraulic jump begins, which is hereafter called HJT. The 3rd forms—after HJT, the hydraulic jump is mainly dominated by gravity, the liquid surface rises and the flow pattern gradually stabilized, which is similar to meniscus during the steady casting and from a certain moment, the state of the flow pattern basically does not change significantly before the nozzle is immersed (although there is a difference of the flow field between the nozzle immersed situation and not immersed situation), that is, the steady liquid level at the moment, is hereafter called SLL. Until the cast end, the form of the hydraulic jump in stage IV also conforms to a stationary hydraulic jump. As a result, some formulas and experiences applicable to hydraulic jumps can be applied to the continuous casting process.

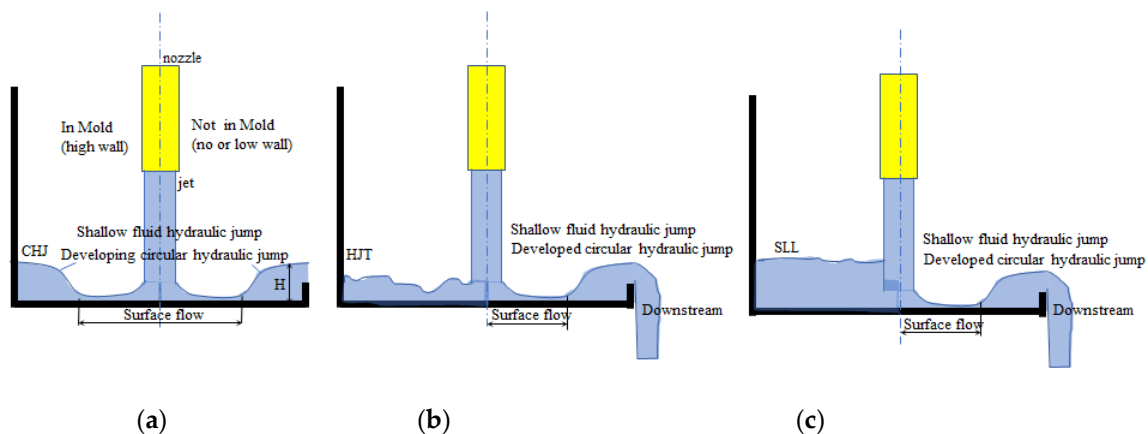


**Figure 2.** Schematic of hydraulic jump evolution in and not in the mold; (a) CHJ; (b) HJT; (c) SLL.

Besides, the hydraulic jump behavior changes due to liquid jet impingement on patterned surfaces with alternating microscale-ribs and cavities [21]. Then, different spring and iron chips arrangement on the dummy bar in the filling process should cause the change of the hydraulic jump.

Therefore, this study presents a quasi-three-dimensional hydraulic model experiment of the transient fluid flow phenomena during the cast start (exactly filling process). The flow field is investigated and optimized by controlling the hydraulic jump behavior with adjusting the spring and iron chips arrangement on the dummy bar. Of course, the properties of water and liquid metal are different. In further work, it is necessary to take into account such physical properties of melts as liquid fluidity, microstructure, and especially the near order at the atomic level.

## 2. Experimental Process

In this paper, a 1:4 hydraulic model experiment is carried out for stages I–II of the continuous casting process, and the geometric size is listed in Table 1. The light path

is designed and shot at 750 frames/s (PHOTRON WX-50 camera, Tokyo, Japan), the triangular prism is placed on the left side of the mold, and the data of the front and side view directions are recorded at the same time as Figure 3a. The plane mirror is placed at 45° in front of the mold, the front and the top view data are captured at the same time as Figure 3b. The obtained quasi-three-dimensional data are helpful to determine the form of the hydraulic jump from different angles, including hydraulic jump heights, the time for the liquid level stable, and the corresponding velocity during the cast start, etc. The velocity data are processed with the open-source software PIVlab (PIVlab 2.53, William Thielicke, Hamburg, Germany) to quantify the change of the hydraulic jump. Experiments for each parameter are done 5–6 times. The durations of CHJ, CHJ to HJT, and HJT to SLL are measured as follows: for the shot at 750 frames/s, the time interval between each two photos is 1/750s, set at the moment when the jet contacts the surface of the dummy bar as the starting point 0, which is the Kth photo, and the CHJ, HJT, and SLL moments are the Lth, Mth, and Nth photos, respectively. The duration of CHJ is from 0 to CHJ, that is, Kth photos to Lth photos, the duration is  $(L-K-1) \times (1/750)$ , the durations of CHJ to HJT and HJT to SLL are measured and calculated in the same way,  $(M-L-1) \times (1/750)$ ,  $(N-M-1) \times (1/750)$ , respectively.

**Table 1.** Geometric parameters of the mold and experimental condition.

Parameter, mm	Inner/Outlet Diameter of Nozzle	Mold Section Size	Mold (Liquid Level) Height Observed
	8/12	50 × 50	50
Experiment No.	Casting speed, $v$ (m/min)	Outlet flow, $Q$ (m <sup>3</sup> /h)	Fr
1	0.8	0.06	1.19 = Fr < 1.7
2	2.4	0.18	3.56 = Fr < 1.7

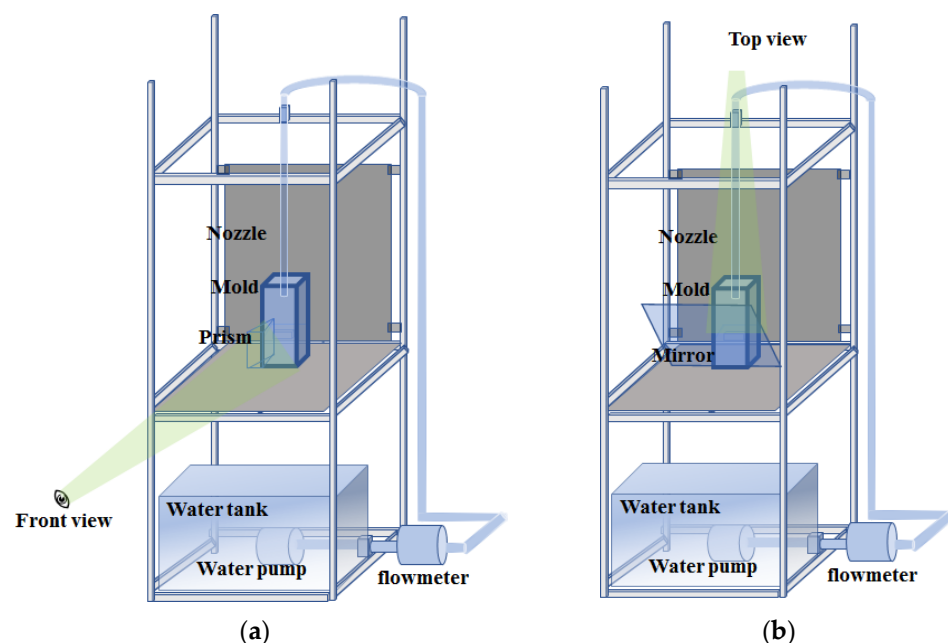


**Figure 3.** Experimental setting. (a) Front view and side view. (b) Top view and front view.

On the one hand, during the filling process, three important physical forms of the hydraulic jump are determined (photos as shown in Figure 4 and explained above in detail); the process is observed until the liquid level height reaches 50 mm (height of the liquid surface/level is lower than the 50 mm until the liquid level steady). On the other hand,  $Fr > 1.7$  is one critical point of the stationary hydraulic jump [22]. Under the two flow regimes divided by the critical point, the common stationary hydraulic jump behavior

should be different during the stage when CHJ disappears until the liquid surface steady. Therefore, two representative casting speeds (0.8 m/min, 2.4 m/min) are selected and the corresponding flow rate of the experiment is obtained, as shown in Table 1.

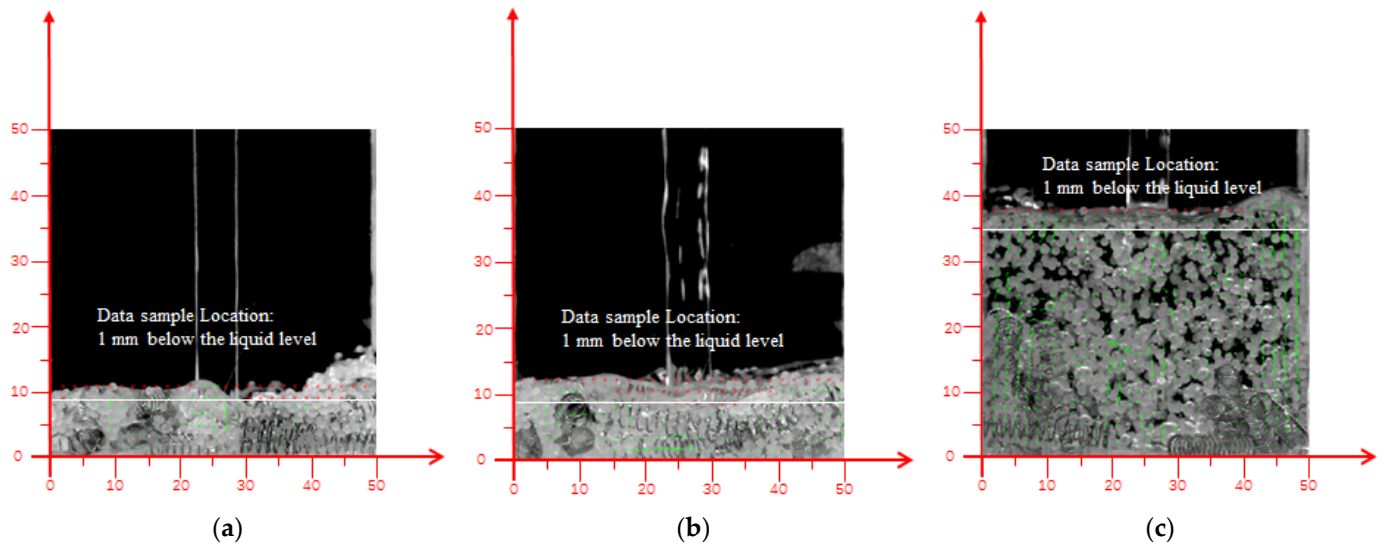


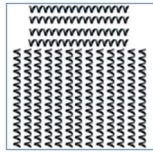
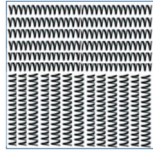
**Figure 4.** Three physical forms of the hydraulic jump (casting speed of 2.40 m/min, mode 4). (a) CHJ. (b) HJT. (c) SLL.

In order to study the effect of the spring and particles arrangement on the initial flow field/hydraulic jump, polystyrene particles are used to simulate the iron chips and serve as tracer particles in this experiment. Laying one layer particles on the dummy bar requires about 2 g polyethylene particles. The ball pen spring is used to replace the spring in actual production. Two types of springs are used here, and the lengths are 25 mm and 35 mm, respectively. A total of 6 different arrangements (modes) are shown in Table 2. The design of the spring arrangement takes into account the relative motion between the springs, the interaction between the fluid and the spring, that is, the gap and the pattern of the spring arrangement is considered; modes 2–5 basically cover the entire dummy bar surface to limit the mutual movement of the spring on the dummy bar surface. Mode 6 increases the gap between springs and mode 1 just covers half of the dummy bar surface. Different modes are used to study the effect of different degrees of freedom on the hydraulic jump behavior.

**Table 2.** Arrangement of springs and particles.

Arrangement of Springs	Mode	Top View	Front View
mode 1: 35 mm			
mode 2: 35 mm			

Table 2. Cont.

Arrangement of Springs	Mode	Top View	Front View
mode 3: 35 mm			
mode 4: 25 mm			
mode 5: 25 mm			
mode 6: 25 mm			

Taking the casting speed of 2.40 m/min, mode 4 as an example, the velocity vector at three moments/physical forms and their analysis position are shown in Figure 4. The flow field in three forms of the hydraulic jump during the filling process is processed by PIVlab. The flow field analysis area selected is rectangular in PIVlab. The selected area is divided into two areas by the fluctuating liquid surface, one part is liquid under the surface, and another is air above the surface. The area not analyzed is indicated by the red cross “×”; in the area analyzed, the velocity vector is indicated by the green arrow “→”.

### 3. Results and Discussion

First, the whole hydraulic jump evolution and its two-dimensional flow field are observed (in Figures 5–8). Second, the velocities at 1 mm below the liquid surface in the three forms of the hydraulic jump are quantitatively analyzed (in Figures 9–12). The value position of the velocity data used in Figures 9–12 at 1 mm below the liquid level is also shown in Figure 4). Finally, the relationship between the spring arrangement, flow, and hydraulic jump are established during the filling process (Figures 13–15).

The flow field in three physical forms of the hydraulic jump of the front view (casting speed of 0.8 m/min, modes 1–6) is shown in Figure 5. The flow formed by the jet moves the spring away from the initial position, then, the initial spring arrangement changes and evolves as the liquid level rises up to the SLL due to buoyancy and the initial velocity of the jet. In CHJ and HJT, the liquid level height and the spring arrangement height are basically the same, that is, the water just submerges the spring, and due to the small amount of liquid, the spring cannot move sufficiently. After HJT, the total amount of liquid increases, the spring is sufficiently buoyant and has enough room to move, and the springs are brought to the liquid surface in some modes, which floats on the liquid surface under the action of buoyancy and surface tension.

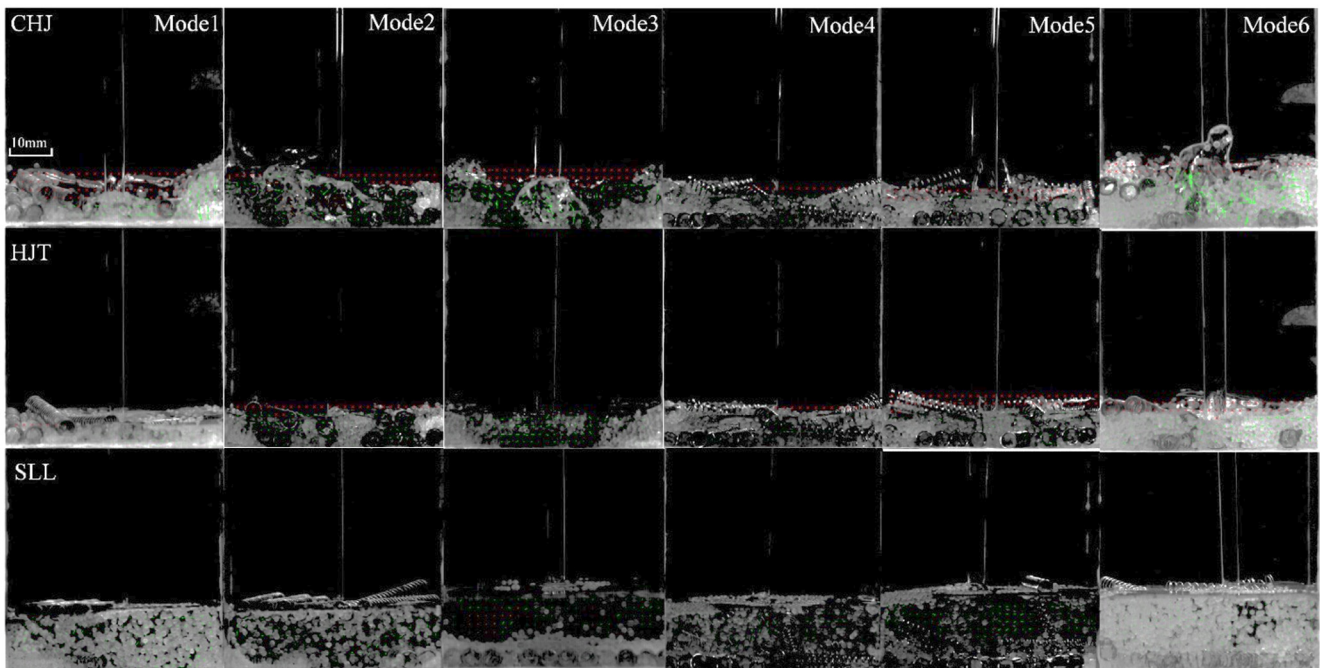


**Figure 5.** The hydraulic jump form and flow field in three physical forms of the hydraulic jump of front view. (casting speed of 0.8 m/min, modes 1–6).

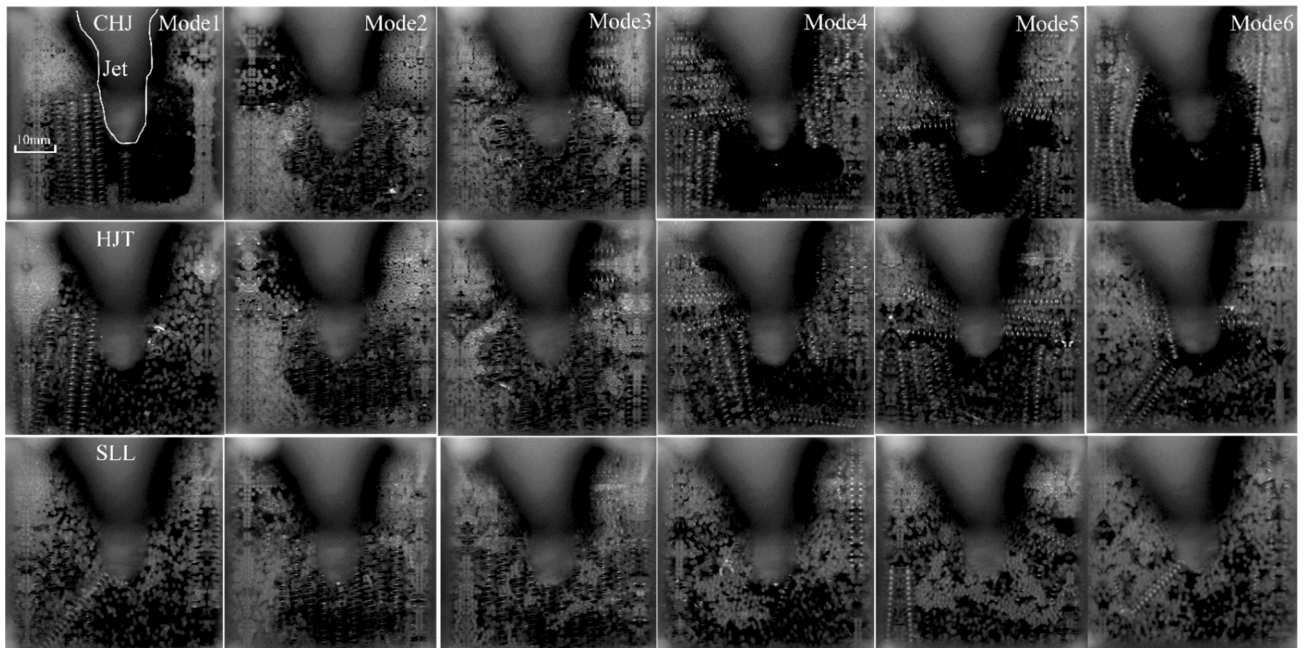


**Figure 6.** The hydraulic jump form and spring and particles arrangement in three physical forms of the hydraulic jump of the top view (casting speed of 0.8 m/min, modes 1–6).

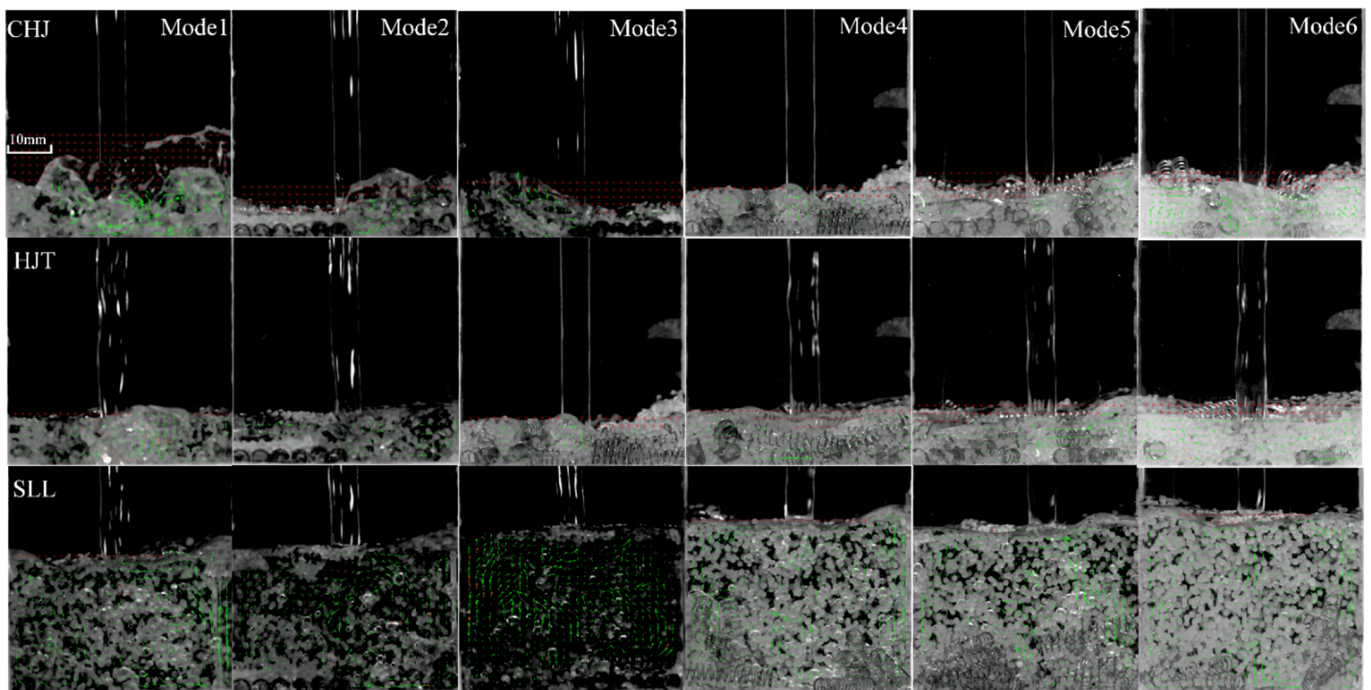


**Figure 7.** The hydraulic jump form and flow field in three physical forms of the hydraulic jump of the front view (casting speed of 2.4 m/min, modes 1–6).

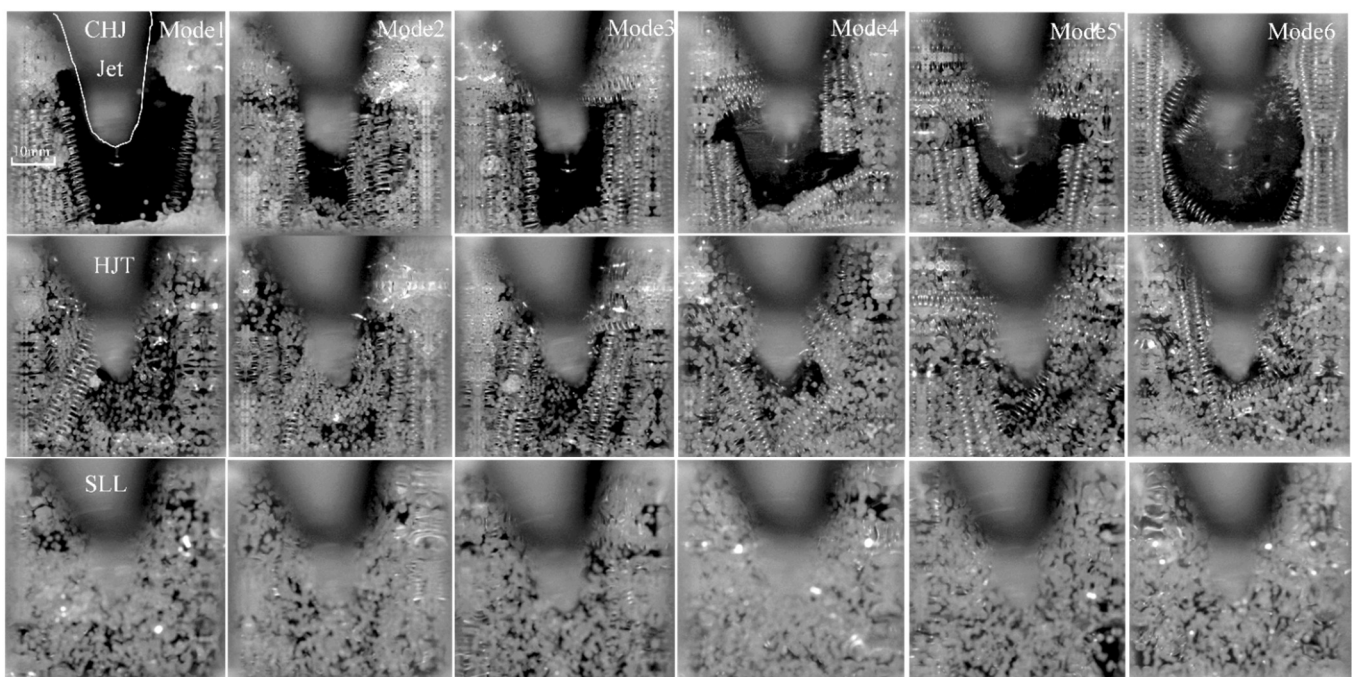


**Figure 8.** The hydraulic jump form and spring and particles arrangement in three physical forms of the hydraulic jump of the top view (casting speed of 2.4 m/min, modes 1–6).

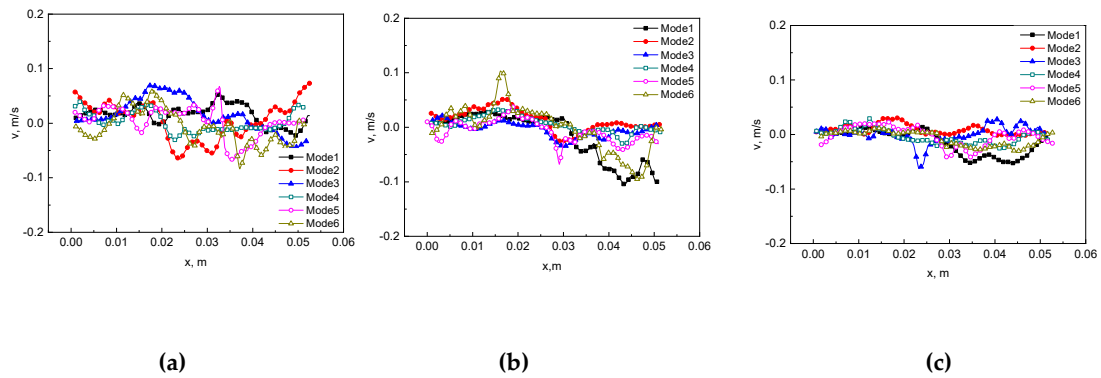


**Figure 9.** The horizontal component of velocity at 1 mm below the liquid surface in three physical forms of the hydraulic jump (casting speed 0.8 m/min). (a) CHJ. (b) HJT. (c) SLL.

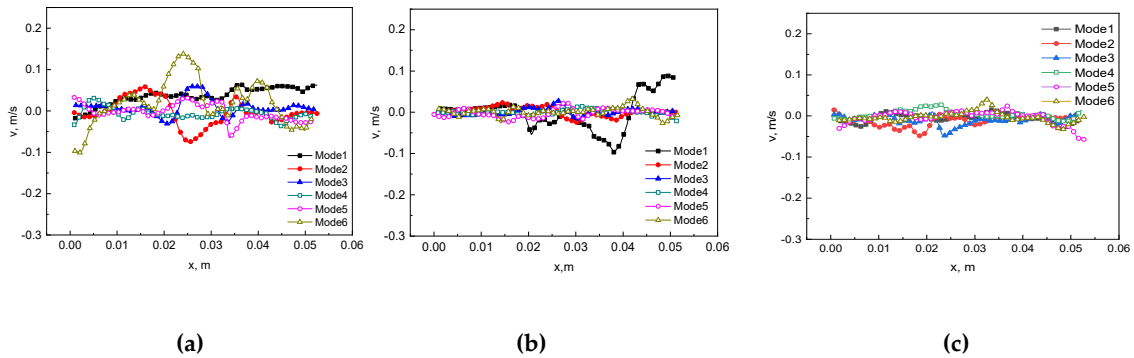


**Figure 10.** The vertical component of velocity at 1 mm below the liquid surface in three physical forms of the hydraulic jump (casting speed 0.8 m/min). (a) CHJ. (b) HJT. (c) SLL.

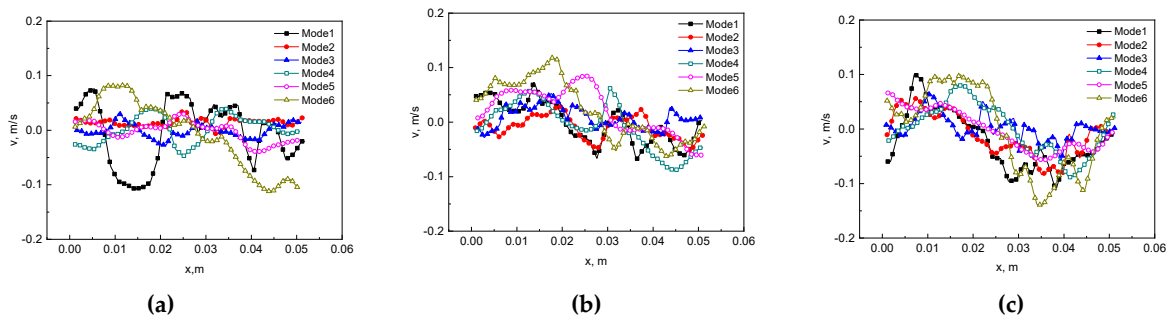


**Figure 11.** The horizontal component of velocity at 1 mm below the liquid surface in three physical forms of the hydraulic jump (casting speed 2.4 m/min). (a) CHJ. (b) HJT. (c) SLL.

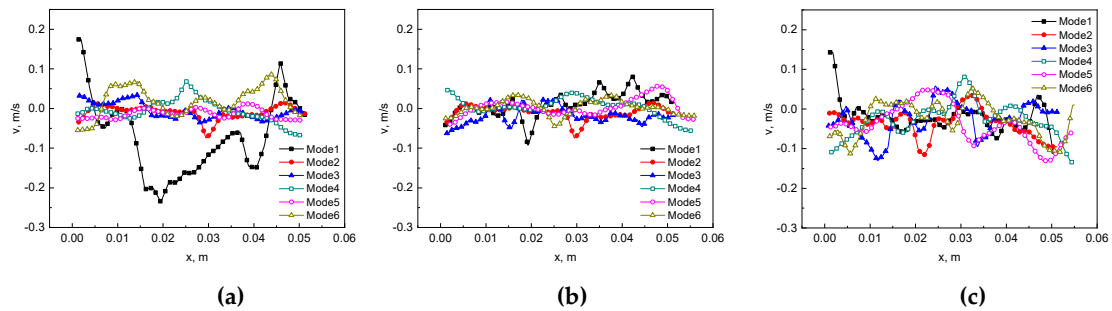


**Figure 12.** The vertical component of velocity at 1 mm below the liquid surface in three physical forms of the hydraulic jump (casting speed 2.4 m/min). (a) CHJ. (b) HJT. (c) SLL.

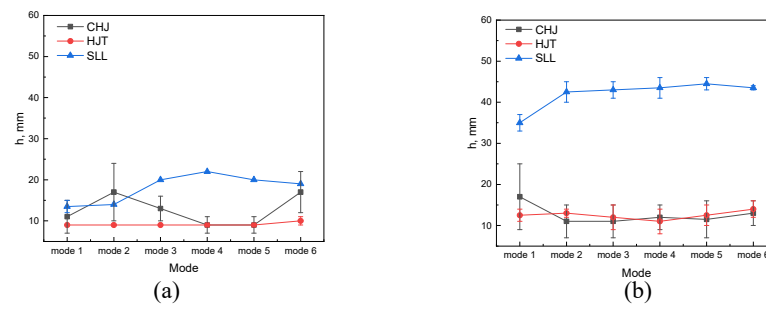


**Figure 13.** The hydraulic jump height of different laying modes in three hydraulic jump forms. (a) 0.8 m/min (b) 2.4 m/min.

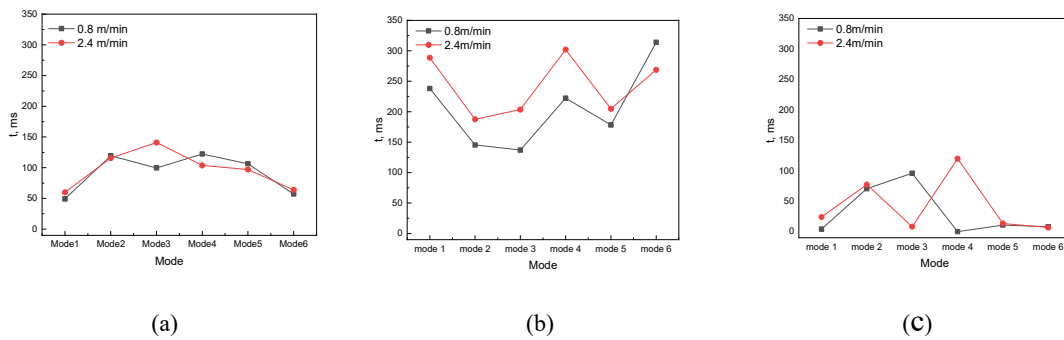


**Figure 14.** Duration of CHJ and CHJ to HJT and HJT to SLL of the different laying mode. (a) CHJ (b) CHJ to HJT (c) HJT to SLL.

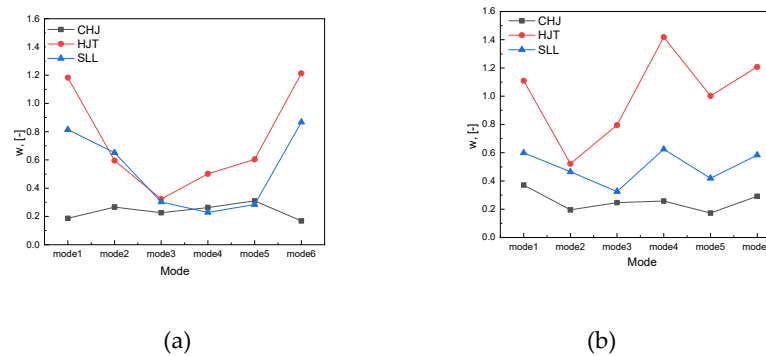


**Figure 15.** Filling coefficient of the different laying mode. (a) 0.8 m/min (b) 2.4 m/min.

The spring and particles arrangement of different modes in the three hydraulic jump forms and changes of arrangement as the liquid level rises after impacted by the jet under the casting speed of 0.8 m/min are shown in Figure 6 (top view, the particles are all in one layer). The distribution of particles can characterize the flow field, which is driven by the hydraulic jump formed after the impact of the jet; and it develops with the flow to the wall. The black area here in the mold center is the surface flow zone (one typical feature of the circular hydraulic jump forms, the surface flow boundary can be characterized by particles). After the impact by the jet, the springs and particles leave the center of the mold and move to the sidewall. The details are as follows:

Modes 1 and 6: The surface flow is affected by the initial arrangement and the wall of the mold. The hydraulic jump develops more quickly than others, the restraint of the spring arrangement for the hydraulic jump is the smallest.

Modes 2 and 3: the initial spring arrangement looks unchanged, the flow is restricted strictly by the initial spring arrangement in CHJ and HJT. The packing morphology of the particles indicates the occurrence of a circular hydraulic jump with a circular surface

flow in the center. Combined with Figure 3 (front view), it can be seen that the spring arrangement of mode 2 has also undergone great changes after HJT. As the liquid level rises, the springs float above the liquid level, but the initial spring arrangement pattern is basically maintained in SLL. The arrangement of mode 3 is almost kept and does not float (no change).

Modes 4 and 5: since the freedom and stability of the arrangement are moderate, the variation of the arrangement is also between the other modes. The arrangement continues to evolve. Except for mode 3, the springs of other modes float above the liquid level in SLL.

Different from the low casting speed, due to the bigger impact of the jet, the arrangements of modes 1–6 are all broken in CHJ; the particles and springs all leave the center, different modes have different surface flow shapes (central black area in the mold) without particles. The surface flow of modes 1 and 6 is the fastest growing, that of modes 4 and 5 is the next, and modes 2 and 3 is the slowest. No springs float above the liquid and they are suspended in the water by buoyancy in SLL. However, regardless of the high or low casting speed (flow rate), the new arrangement formed by evolution has strong consistency or heritability with the initial arrangement (as shown in Figures 7 and 8).

The velocity at 1 mm below the liquid surface in the three forms of the hydraulic jump under the two casting speeds (0.8 m/min, 2.4 m/min) is shown in Figures 9–12. It is an important index for the filling process.

The horizontal component of velocity at 1 mm below the liquid surface in three physical forms of the hydraulic jump (casting speed 0.8 m/min) is shown in Figure 9. The rightward velocity is defined as a positive direction (x direction). It can be seen that in modes 1–6, as the free surface gradually stabilizes, overall, the velocity near the free surface decreases; free surface fluctuations of CHJ are the largest among the three forms (CHJ, HJT, and SLL); in HJT, the symmetric flows come back to fill up the cavity (surface flow) formed by the hydraulic jump, and flows of modes 1–6 have the similar trend; in SLL, the flow pattern is similar to that of HJT and the velocity decreases, even the asymmetric mode 1 with the largest degree of freedom begins to form a symmetric flow, consistent with the other modes. This quantitatively verifies the influence of the spring arrangement on the hydraulic jump.

The vertical component of velocity at 1 mm below the liquid surface in three physical forms of the hydraulic jump (casting speed 0.8 m/min) is shown in Figure 10. The downward velocity is defined as the positive direction (y direction). The conclusions for the vertical components are consistent with those for the horizontal components. Free surface fluctuations of CHJ are the largest among the three forms (CHJ, HJT, and SLL); in HJT and SLL, that of modes 1–6 fluctuate and basically decrease. Combined with Figures 5, 9 and 10, it is a double vortex flow in HJT and SLL.

The horizontal component and vertical component of velocity at 1 mm below the liquid surface in three physical forms of the hydraulic jump (casting speed 2.4 m/min) are shown in Figures 11 and 12. It is similar to the case of the casting speed 0.8 m/min, but due to the larger casting speed (initial flow rate), the stability of the liquid level is more difficult and the fluctuation is larger. The flow pattern of the symmetrical backflow is more obvious. Especially, modes 1 and 6, because their arrangements are very small in terms of space constraints, it fluctuates far more than other modes in CHJ. In addition, since the liquid level rises quickly, there is sufficient room for the flow to develop. In SLL, four vortices are formed under the liquid surface (seen in Figure 7).

The liquid level height of different modes at two different casting speeds in three hydraulic jump forms is shown in Figure 13. It can be seen that the average liquid level height increases with the increase of the casting speed in general, and the liquid level height in HJT has little relationship with the mode/spring arrangement.

At 0.8 m/min casting speed, the liquid level/height of the hydraulic jump changes as follows:

CHJ: the hydraulic jump height/depth of modes 4 and 5 is the lowest and about 9 mm; the maximum height of modes 1, 2, 3, and 6 can reach 15–18 mm.

HJT: There is no obvious difference in the overall liquid profile among modes 1–6; and the average heights of the liquid surface are almost the same in modes 1–6, about 9 mm.

SLL: the liquid level is relatively smooth (but it does not mean the fluctuation velocity value around the liquid surface is small), with a height of about 15–22 mm.

At 2.4 m/min casting speed, the liquid level/height of the hydraulic jump changes as follows:

The flow field at the high casting speed (2.4 m/min) is similar to that at the low casting speed (0.8 m/min), but obviously as the flow rate increases, the velocity in the mold increases and the liquid level rises fast.

CHJ: the average hydraulic jump height of modes 2–6 is low and about 13 mm; the maximum height of mode 1 can reach 26 mm.

HJT: There is no obvious difference in the overall liquid profile among modes 1–6; and the average heights of the liquid surface are almost the same in modes 1–6, about 11–13 mm.

SLL: the liquid level is also relatively smooth (but it does not mean the fluctuation velocity value around the liquid surface is small), with a height of about 44 mm, except mode 1 is 35 mm.

At a low casting speed of 0.8 m/min: the liquid level height in CHJ is the height of the the circular hydraulic jump (it is the height after jump; the center of the mold is a cavity and very thin liquid film here, that is, surface flow), the heights of modes 1, 2, 3, and 6 in CHJ are high, and they even exceed the liquid level height in SLL. Modes 4 and 5 are relatively low, which is almost the same as that in HJT, then the kinetic energy loss is smallest, that is, if the liquid level height is low in CHJ, then the liquid level height is high in SLL. The liquid level increases with the time and reaches the highest in SLL. At a high casting speed of 2.4 m/min: The liquid level of modes 2–6 is basically the same in all three forms, while the liquid level of mode 1 rises in CHJ and decreases obviously in SLL. The liquid level of different modes in HJT at the two casting speeds are almost the same—all modes have a similar trend. It can generally be attributed to the influence of the spring arrangement and characteristics of the hydraulic jump in the filling process.

The duration of the three transition processes of the hydraulic jump (CHJ, HJT, and SLL) is another important parameter. The duration of CHJ for modes 1 and 6 is half of the other modes; the flow rate/casting speed has little effect on the duration, and the duration of different modes is basically the same at the two casting speeds, as shown in Figure 14a. CHJ to HJT is a transitional process from a circular hydraulic jump to a common stationary hydraulic jump, the duration of CHJ to HJT, as shown in the Figure 14b. In this process, the duration of different modes is also basically similar at the two casting speeds and increases with the increase in flow. HJT to SLL is a common stationary hydraulic jump (two or four vortices forms and the liquid level relatively stable), duration of HJT to SLL, as shown in the Figure 14c. The duration of CHJ depends entirely on the spring arrangement (spring arrangement varies after the hitting by jet). The duration of CHJ to HJT increases with the flow and also depends on the spring arrangement. The duration of HJT to SLL also depends on the spring arrangement. It is clarified that designing different arrangements can indeed adjust the hydraulic jump behavior. However, these two indicators cannot yet determine which.

In order to better characterize which kind of laying (modes 1–6) is beneficial to the filling process, a filling coefficient  $w$  (nondimensional velocity) is set.

$$w = |v_F| / |v_{ery}| \quad (1)$$

$|v_F|$ —the absolute value average of fluctuation velocity at liquid level (the average velocity at 1 mm below the liquid surface) in CHJ, HJT, and SLL,  $|v_R|$ —the absolute value of the average liquid level rise velocity in CHJ, HJT, and SLL.  $v_R =$  (the average height of liquid level in CHJ, HJT, SLL)/(duration from start point to CHJ, HJT, SLL), the average height can be obtained from Figures 5 and 7 (front view).

An increase in the filling coefficient  $w$  indicates an increase in fluctuation or a decrease in liquid level rise velocity. The flow field for the filling process needs to be stable and fast to fill the mold. The smaller the filling coefficient, the more the filling process meets the metallurgical goal. The filling coefficient  $w$  applies to the entire filling process before stage III. Additionally,  $w$  has a relatively obvious correlation with flow and spring arrangement (shown in Figure 15).

At a low casting speed of 0.8 m/min:  $w$  of modes 1 and 6 in CHJ is different from that of the other two forms (HJT and SLL); and  $w$  of modes 2–5 has similar laws in the three forms (CHJ, HJT, and SLL).  $w$  of modes 3–5 is small in CHJ and SLL,  $w$  of mode 2, 4, and 5 increases significantly in HJT. At a high casting speed of 2.4 m/min: the law of  $w$  in the three forms basically obeys the mode (arrangement).  $w$  of modes 1, 4, and 6 is large, while  $w$  of modes 2, 3, and 5 is relatively small.

In general,  $w$  is the largest at HJT, followed by SLL, and CHJ is the smallest.  $w$  is small for closely arranged modes, while  $w$  increases for loosely and unstable modes; the change of  $w$  in CHJ is smaller than that in HJT and SLL for all modes. The different spring arrangements really affect the hydraulic jump. Modes 2, 4, and 5 are also good performance. At a low casting speed of 0.8 m/min, only the initial arrangement of mode 3 is kept. The best operation condition is mode 3 at a low casting speed. Its structure is tight enough and stable.

For the hydraulic jump, surface tension plays the role in CHJ, gravity plays the role in SLL, and from CHJ to HJT, surface tension decreases, gravity increases; this process is a dynamic balance between surface tension and gravity [18,19]. The HJT is the critical transition node from which gravity exceeds surface tension.

Meanwhile, according to the visualization results, it can be seen that the initial spring arrangement forms a new arrangement structure after being impacted by jet, and the evolution process of this new structure is affected by the initial arrangement and the jet. Then, the new arrangement influences the hydraulic jump.

#### 4. Conclusions

This work investigates the transient fluid flow phenomena during the filling process of the cast start. The relationship between the continuous casting process and the hydraulic jump phenomenon is established. The casting process in the mold is divided into four stages (I–IV) from the beginning to the end of continuous casting. The filling process involves stages I–II, the circular hydraulic jump occurs firstly, then it turns into the common stationary hydraulic jump. The three key states of the hydraulic jump phenomenon during the filling process are determined, namely CHJ, HJT, and SLL. The conclusions are as follows:

1. The height of the hydraulic jump/liquid level at different casting speeds in the three states is obtained. The arrangement and casting speed both have little effect on the height in HJT, which is almost the same in each mode; and the height in SLL reaches highest.
2. The duration for CHJ and CHJ to HJT is obtained. The arrangement and casting speed both have an effect on the duration, and the duration increases with the increase in the casting speed. The duration of CHJ modes 1 and 6 is half of the other modes. The duration of CHJ to HJT increases with the flow and also depends mostly on the spring arrangement.
3. The filling coefficient  $w$  is proposed.  $w$  is the largest at HJT, followed by SLL, and CHJ is the smallest.  $w$  is small for closely arranged modes, while  $w$  increases for loosely and unstable modes; the change of  $w$  in CHJ is smaller than that in HJT and SLL. The different spring arrangements really affect the hydraulic jump. At a low casting speed of 0.8 m/min, only mode 3 maintains the initial arrangement and it is the best operation condition.

**Author Contributions:** Conceptualization, J.C.; methodology, J.C.; validation, J.C. and L.Z.; formal analysis, J.C. and L.Z.; investigation, J.C., L.Z., J.Z., P.C., G.L. and F.W.; resources, J.C.; data curation, J.C. and L.Z.; writing—original draft preparation, J.C. and L.Z.; writing—review and editing, J.C.; supervision, J.C.; project administration, J.C.; funding acquisition, J.C. All authors have read and agreed to the published version of the manuscript.

**Funding:** This paper is financially supported by National Natural Science Foundation of China [51604076] and [U1560207].

**Data Availability Statement:** Data sharing is not applicable.

**Acknowledgments:** Thank you for Qiang Wang. The paper is financially supported National Natural Science Foundation of China [U1560207] and the reviewed and edited by him.

**Conflicts of Interest:** The authors declare no conflict of interest.

## References

1. Watanabe, T.; Omura, K.; Konishi, M.; Watanabe, S.; Furukawa, K. Mold level control in continuous caster by neural network model. *ISIJ Int.* **1999**, *39*, 1053–1060. [[CrossRef](#)]
2. Zhang, L.F.; Thomas, B.G. State of the Art in Evaluation and Control of Steel Cleanliness. *ISIJ Int.* **2003**, *43*, 271–291. [[CrossRef](#)]
3. Hintikka, S.; Konttinen, J.; Leivisk, K.; Tolvanen, M. Optimization of molten steel flow in continuous casting mold. In Proceedings of the Optimization of Molten Steel Flow in Continuous Casting Mold, Toronto, ON, Canada, 5 April 1992.
4. Cramer, A.; Eckert, S.; Galindo, V.; Gerbeth, G.; Willers, B.; Witke, W. Liquid metal model experiments on casting and solidification processes. *J. Mater. Sci.* **2004**, *39*, 7285–7294. [[CrossRef](#)]
5. Timmel, K.; Kratzsch, C.; Asad, A.; Schurmann, D.; Schwarze, R.; Eckert, S. Experimental and Numerical Modeling of Fluid Flow Processes in Continuous Casting: Results from the LIMMCAST-Project. *Mater. Sci. Eng.* **2017**, *228*, 012019. [[CrossRef](#)]
6. Chen, J.; Su, Z.; Li, D.; Wang, Q.; He, J. Flow Behavior in the Slab Mold under Optimized Swirling Technology in Submerged Entry Nozzle. *ISIJ Int.* **2018**, *58*, 1242–1249. [[CrossRef](#)]
7. Chattopadhyay, K.; Isac, M.; Guthrie, R.I.L. Physical and Mathematical Modelling to Study the Effect of Ladle Shroud Misalignment on Liquid Metal Quality in a Tundish. *ISIJ Int.* **2011**, *51*, 759–768. [[CrossRef](#)]
8. Chen, Y.; Zhang, L.; Yang, S.; Li, J. Water Modeling of Self-Braking Submerged Entry Nozzle Used for Steel Continuous Casting Mold. *JOM* **2012**, *64*, 1080–1086. [[CrossRef](#)]
9. Deng, X.; Wang, X.; Li, L.; Ji, C.; Zeng, Z.; Tian, Z. Surface Cleanliness Evaluation on Transition Slabs of IF Steel and water Modeling of Mold Level Ladle Change Process. In Proceedings of the 17th National Steelmaking, Hangzhou, China, 5 May 2013; p. 1373.
10. Huang, Z.; Shuai, Y.; Ren, C.; Yang, Y.; Sun, J.; Wang, J.; Yang, Y. Effects of internal structures on mass transfer performance of jet bubbling reactor. *Chem. Eng. Process.* **2022**, *175*, 108936. [[CrossRef](#)]
11. Gregorc, J.; Kunavar, A.; Sarler, B. RANS versus Scale Resolved Approach for Modeling Turbulent Flow in Continuous Casting of Steel. *Metals* **2021**, *11*, 1140. [[CrossRef](#)]
12. Liu, F.; Zhou, H.; Zhang, L.; Ren, C.; Zhang, J.; Ren, Y.; Chen, W. Effect of Temperature and Multichannel Stopper Rod on Bubbles in Water Model of a Steel Continuous Caster. *Steel Res. Int.* **2021**, *92*, 2100067. [[CrossRef](#)]
13. Wang, Y.F.; Zhang, L.F. Transient Fluid Flow Phenomena during Continuous Casting: Part I—Cast Start. *ISIJ Int.* **2010**, *50*, 1777–1782. [[CrossRef](#)]
14. Wang, Y.F.; Zhang, L.F. Transient Fluid Flow Phenomena during Continuous Casting: Part II—Cast Speed Change, Temperature Fluctuation, and Steel Grade Mixing. *ISIJ Int.* **2010**, *50*, 1783–1791. [[CrossRef](#)]
15. Zhang, Q.Y.; Wang, L.T.; Wang, X.H.; Li, H.; Wang, W.J. Non-metallic inclusion distribution in surface layer of IF steel slabs. *Iron Steel Res. Int.* **2008**, *15*, 70–74. [[CrossRef](#)]
16. Chakroborty, S.; Sahai, Y. Mathematical modeling of transport phenomena in continuous casting tundishes part 1. Transient effects during ladle transfer operations. *Ironmak. Steelmak.* **1992**, *19*, 479.
17. Huang, X.; Thomas, B.G. Modeling of steel grade transition in continuous slab casting processes. *Metall. Mater. Trans. B* **1993**, *24*, 379–393. [[CrossRef](#)]
18. Bhagat, R.K.; Jha, N.K.; Linden, P.F.; Wilson, D.I. On the origin of the circular hydraulic jump in a thin liquid film. *J. Fluid Mech.* **2018**, *851*, R5. [[CrossRef](#)]
19. Hossein, A.; Hossein, A.; Claas, E.; Reinhold, K.; Ahmadrza, P.; Wilko, R. Role of gravity and capillary waves in the origin of circular hydraulic jumps. *Phys. Rev Fluids* **2019**, *4*, 114002.
20. Bush, J.W.M.; Aristoff, J.M.; Hosoi, A.E. An experimental investigation of the stability of the circular hydraulic jump. *J. Fluid Mech.* **2006**, *558*, 33–52. [[CrossRef](#)]
21. Johnson, M.; Maynes, D.; Crockett, J. Experimental characterization of hydraulic jump caused by jet impingement on micro-patterned surfaces exhibiting ribs and cavities. *Exp. Therm. Fluid Sci.* **2014**, *58*, 216–223. [[CrossRef](#)]
22. Khatsuria, R.M. *Hydraulics of Spillways and Energy Dissipaters*; Marcel Dekker: New York, NY, USA, 2005.